46th AIAA Aerospace Sciences Meeting and Exhibit
7 - 10 January 2008, Reno, Nevada

AIAA 2008-18

Unsteady Optimization Using a Discrete Adjoint Approach Applied to Aeroacoustic Shape Design

Markus P. Rumpfkeil* and David W. Zingg †
University of Toronto Institute for Aerospace Studies
4925 Dufferin Street, Toronto, ON, M3H 5T6, Canada

In this paper, shape optimization is used to minimize aerodynamic noise in an unsteady trailing-edge flow. First, a generic time-dependent optimal design problem is introduced and the derivation of the discrete adjoint equations in a general approach is outlined. The presented framework is then applied to a time-dependent laminar flow past an acoustically compact airfoil. The results show a significant reduction of up to 94 percent in the total radiated acoustic power with reasonable computational cost using fifteen shape design variables.

Nomenclature

a_∞	Free stream speed of sound	c	Chord length
$\bar{C}_L$	Mean lift coefficient	$\bar{C}_D$	Mean drag coefficient
I^n	Objective function at time step n	J	Objective function
$\frac{\partial J}{\partial Y}$	Gradient of objective function	M_∞	Free stream Mach number
N	Total number of time steps	N^*	Number of coarse time steps
p	Pressure	Q^n	Flow variables at time step n
$\mathcal{R}^n$	Unsteady flow residual	$(\nabla_{Q^n}\mathcal{R}^n)^T$	Transpose of the unsteady flow Jacobian
R	Flow residual	$\mathcal{R}e$	Reynolds number
$\mathcal{S}$	Airfoil surface	t	Time
T	Final time	u_∞	Free stream velocity
Y	Design variables	$\mathcal{L}$	Lagrangian
ρ_∞	Free stream density	ψ^n	Adjoint variables at time step n
Δt	Time discretization step	Δt^*	Coarse time discretization step

I. Introduction and Motivation

The use of steady-state aerodynamic optimization methods in the computational fluid dynamics (CFD) community is fairly well established.[1–4] In particular the use of adjoint methods, which has been pioneered by Jameson[5] for steady aeronautical design optimization, has proved to be very beneficial since its cost is independent of the number of design variables.

The application of numerical optimization to airframe-generated noise, however, has not received as much attention, but with the significant quieting of modern engines, airframe noise now competes with engine noise.[6] Thus airframe-generated noise is an important component of the total noise radiated from commercial aircraft, especially during aircraft approach and landing, when engines operate at reduced thrust, and airframe components (such as high-lift devices) are in the deployed state.[7] Future Federal Aviation Administration noise regulations, the projected growth in air travel and the increase in population density

*Ph.D Candidate, Student Member AIAA, markus@oddjob.utias.utoronto.ca
†Professor, Tier I Canada Research Chair in Computational Aerodynamics, Associate Fellow AIAA, http://goldfinger.utias.utoronto.ca/∼dwz/

near airports will require future civil aircraft to be substantially quieter than current ones. Consequently, the attempt to understand and reduce airframe noise has become an important research topic.[8]

Optimal control techniques for unsteady flows are needed in order to be able to reduce airframe-generated noise. This paper presents a general framework to calculate the gradient in a nonlinear unsteady flow environment via the discrete adjoint method. The presented framework is then applied to an aerodynamic noise reduction problem involving unsteady laminar trailing-edge flow similar to one presented by Marsden *et al.*[9]

II. Formulation of the Discrete Time-dependent Optimal Control Problem

In the following we assume that we control an unsteady flow in the time interval $[0, T]$ with an initial flow solution Q^0 at $t = 0$. In this section we use the implicit Euler time-marching method to discretize the governing equations in time. This is not a restriction, since it is straightforward to modify the equations to use any other time-marching method (e.g. see the Appendix for the derivation with the second-order backwards difference (BDF2) time-marching method, which is used to obtain the results).

We introduce a cost function

$$J = \sum_{n=1}^{N} I^n(Q^n, Y), \tag{1}$$

where the function $I^n = I^n(Q^n, Y)$ depends on the time-dependent flow solution Q^n and design variables Y. N can be calculated from the relation $T = N\Delta t$, where Δt is the chosen time discretization step. We then assume that $R = R(Q^n, Y)$ contains the spatially discretized convective and viscous fluxes as well as the boundary conditions and that

$$\mathcal{R}^n(Q^n, Q^{n-1}, Y) := \frac{Q^n - Q^{n-1}}{\Delta t} + R(Q^n, Y) = 0 \tag{2}$$

defines implicitly the time-dependent flow solution Q^n for $n = 1, \ldots, N$. It does not matter how one solves equation (2) as long as $\mathcal{R}^n = 0$ for all n, since this is the requirement for the following derivation.

The task of minimizing the cost function J subject to $\mathcal{R}^n = 0$ for all n can now be written as an unconstrained optimization problem of minimizing the Lagrangian function

$$\mathcal{L} = \sum_{n=1}^{N} I^n(Q^n, Y) + \sum_{n=1}^{N} (\psi^n)^T \mathcal{R}^n(Q^n, Q^{n-1}, Y) \tag{3}$$

with respect to $Q^1, \ldots, Q^N$ and $\psi^1, \ldots, \psi^N$, where $\psi^1, \ldots, \psi^N$ are the N vectors of Lagrange multipliers. A necessary condition for an extremal is that the gradient of $\mathcal{L}$ with respect to $Q^1, \ldots, Q^N$ and $\psi^1, \ldots, \psi^N$ should vanish. Since we start with Q^0 and calculate the states $Q^1, \ldots, Q^N$ using the constraints given by equation (2), we ensure that $\nabla_{\psi^n}\mathcal{L} = 0$ for $n = 1, \ldots, N$ automatically. The Lagrange multipliers ψ^n must now be chosen such that $\nabla_{Q^n}\mathcal{L} = 0$ for $n = 1, \ldots, N$, which leads to

$$0 = \nabla_{Q^n} I^n + (\psi^n)^T \nabla_{Q^n} \mathcal{R}^n + (\psi^{n+1})^T \nabla_{Q^n} \mathcal{R}^{n+1} \qquad \text{for} \quad n = 1, \ldots, N\text{–}1 \tag{4}$$

$$0 = \nabla_{Q^N} I^N + (\psi^N)^T \nabla_{Q^N} \mathcal{R}^N. \tag{5}$$

This can be written equivalently as

$$\psi^N = -\left((\nabla_{Q^N} \mathcal{R}^N)^T\right)^{-1} (\nabla_{Q^N} I^N)^T \tag{6}$$

$$\psi^n = -\left((\nabla_{Q^n} \mathcal{R}^n)^T\right)^{-1} \left[(\nabla_{Q^n} I^n)^T + (\nabla_{Q^n} \mathcal{R}^{n+1})^T \psi^{n+1}\right] \qquad \text{for} \quad n = N\text{–}1, \ldots, 1. \tag{7}$$

Since $Q^1, \ldots, Q^N$ have been calculated from the current iterate of Y, the Lagrange multipliers ψ^n can be calculated recursively backwards from the terminal boundary condition (6) using (7). The system of equations (6) and (7) is known as the system of adjoint equations for the model (2), or as the adjoint model. In this context, the Lagrange multipliers are also known as the adjoint variables.

Finally, one can evaluate the gradient of J with respect to the design variables Y, which can then be used in a gradient-based optimization algorithm such as BFGS[10–13] to find the optimum:

$$\frac{\partial J}{\partial Y} = \frac{\partial \mathcal{L}}{\partial Y} = \sum_{n=1}^{N} \nabla_Y I^n(Q^n, Y) + \sum_{n=1}^{N} (\psi^n)^T \nabla_Y R(Q^n, Y). \tag{8}$$

In summary, the gradient is determined by the solution of the adjoint equations in reverse time from the terminal boundary condition and the partial derivatives of the flow residual and objective function with respect to the design variables (while Q^n is held constant). One can also see that the computational costs of unsteady optimization problems are directly proportional to the desired number of time steps and (almost) independent of the number of design variables.

III. The Aerodynamic Noise Reduction Problem

We now present an unsteady aerodynamic noise reduction problem which applies the above framework in practice. The airfoil geometry, which is a shortened version of the airfoil used in experiments by Blake,[14] is shown in Figure 1. This geometry is very similar to the one used by Marsden *et al.*[9] in their noise minimization using a surrogate management framework. The airfoil chord is 10 times its thickness, the free stream Mach number is $M_\infty = 0.2$ with a Reynolds number of $\mathcal{R}e = 10,000$, and the angle of attack is $0°$.

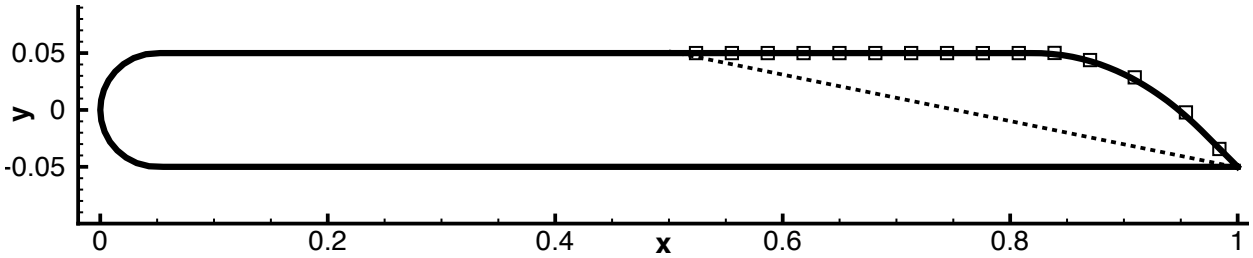

Figure 1: Blake airfoil used in unsteady laminar flow problem with the thickness constraint line (dashed). The right half of the upper surface is allowed to deform and the fifteen B-spline control points which are used as design variables are shown as squares.

For unsteady laminar flow past an airfoil at low Mach number, the acoustic wavelength associated with the vortex shedding is typically long relative to the airfoil chord.[9] The noise generation from such an acoustically compact airfoil can be expressed using Curle's extension to the Lighthill theory[15] and a cost function J, which is proportional to the total radiated acoustic power can be derived:[16]

$$J = \overline{\left(\frac{\partial}{\partial t}\int_{\mathcal{S}} n_j p_{1j}(y,t)ds\right)^2} + \overline{\left(\frac{\partial}{\partial t}\int_{\mathcal{S}} n_j p_{2j}(y,t)ds\right)^2}. \tag{9}$$

Here, p_{ij} is the compressive stress tensor, n_j are the normalized components of the outward normal to the airfoil surface $\mathcal{S}$, and y is the airfoil surface position vector. The overbar denotes time-averaging over the chosen time interval, and repeated indices follow the usual Einstein summation convention. The radiation in this case is of dipole type, caused by the fluctuating lift and drag forces; the reader is referred to Wang *et al.*[17] for more details on airfoil self-noise due to vortex shedding.

The geometry of the airfoil is described with cubic B-spline curves,[4] which means that some of the y-coordinates of the B-spline control points in the upper right half of the airfoil can easily be used as shape design variables (see Figure 1). Since the cost of our adjoint approach is independent of the number of design variables, we decided to use considerably more shape design variables than the five that Marsden *et al.*[9] could afford in their study using a surrogate management framework. We use fifteen shape design variables in this research, thus giving the airfoil more freedom in the design space to take the most beneficial shape as given by the BFGS optimizer.[18,19] However, we impose thickness constraints via a quadratic penalty method to ensure that the airfoil has a certain minimum thickness. We apply the same minimum thickness as imposed by Marsden *et al.*, which is given by a straight line connecting the left edge of the deformation region and the trailing edge, as shown in Figure 1.

We use a C-mesh with 298×95 nodes, which is a good compromise between the accuracy of the flow solution and the computational effort required. In order to solve the underlying two-dimensional unsteady compressible thin-layer Navier-Stokes equations in non-dimensional form we use our flow solver PROBE[20] with the second-order accurate BDF2 time-marching method. The spatial discretization of the steady flow residual $R = R(Q^n, Y)$ is the same as that used in ARC2D.[21] It consists of second-order centered-difference operators with second- and fourth-difference scalar artificial dissipation. We use an inexact Newton strategy[20,22] to drive the discretized unsteady flow residual $\mathcal{R}^n$ to 10^{-12} at each time step n. The main com-

ponents of this strategy include the matrix-free generalized minimum residual (GMRES) method[23] and an incomplete lower-upper factorization[24] ILU(k) right preconditioner with a fill level of $k = 4$ to inexactly solve the linear system, which results from applying Newton's method to equation (2). The preconditioner is based on a first-order approximation of the flow Jacobian matrix, and the matrix-vector products required at each GMRES iteration are formed with first-order finite differences. The non-dimensionalization is accomplished with the following scaling parameters: the free stream density ρ_∞, the airfoil chord c as a length scale, the free stream speed of sound a_∞ as a velocity scale, and c/a_∞ as a time scale. Our Reynolds number of $10,000$ is based on the free stream velocity u_∞ and the chord length c. Marsden *et al.* used a very similar scaling to present their results, although they used u_∞ as the velocity scale. In order to convert the objective function value from our scaling to Marsden's scaling we have to divide it by $(M_\infty)^6$, and we have to multiply our non-dimensionalized time by M_∞ to be able to compare it to Marsden's non-dimensionalized time. For the remainder of this paper we will report all our results with Marsden's scaling to ease comparisons.

The Bi-CGSTAB algorithm[25] is used to solve the linear systems in the adjoint equations with an absolute convergence tolerance of 10^{-6} and right preconditioning with ILU(5) is applied to accelerate convergence. We found Bi-CGSTAB to be about fifty percent faster in solving the unsteady adjoint equations than GMRES, which we still use in our unsteady flow solves as mentioned above because there are no significant computational savings by using Bi-CGSTAB for the few linear iterations we have to use per nonlinear (outer) iteration. However, for a steady-state adjoint problem Bi-CGSTAB works not nearly as well and we are using GMRES instead. The reason for this is most likely accounted for by the fact that $(\nabla_{Q^n}\mathcal{R}^n)^T$ is more diagonally dominant than the transpose of the steady flow Jacobian $(\nabla_Q R)^T$ due to the extra terms on the diagonal, which makes this matrix more suited for the use of Bi-CGSTAB.

We also found that the algebraic grid movement algorithm used by Nemec and Zingg[26] is not capable of dealing with the occasional fairly large shape changes. Thus we use a quasi-linear elasticity mesh movement method[27,28] with three increments.

IV. Results

The laminar flow around the original Blake airfoil exhibits unsteady vortex shedding, which leads to an oscillatory cost function as shown in Figure 2 using a time step size of $\Delta t = 0.005$. The agreement between our cost function for the original Blake airfoil and the one shown in Marsden *et al.*[9] is reasonably good, even though our grid is about five times coarser.

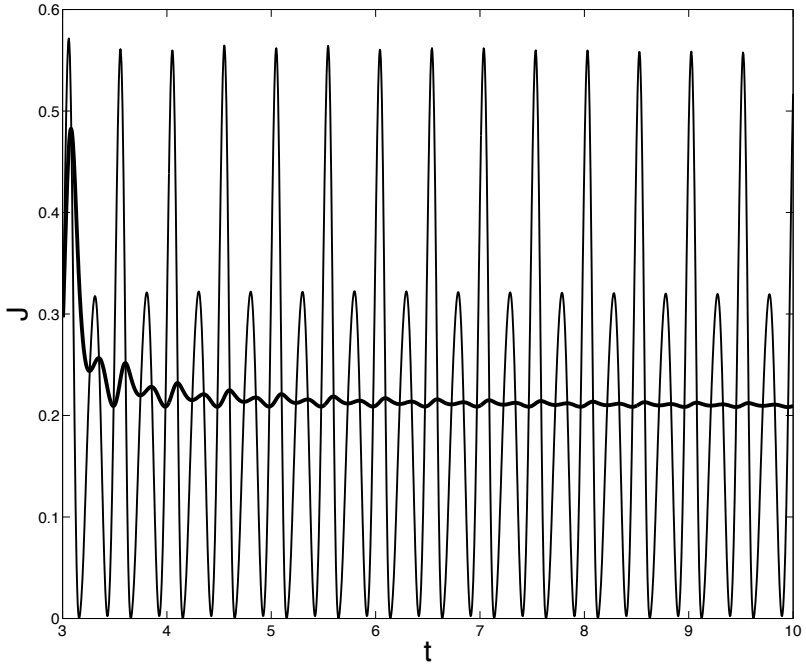

Figure 2: Instantaneous (thin line) and time-averaged (thick line) cost function for the original Blake airfoil vs. time.

In the actual optimization runs we use the discrete version of the time-averaged cost function given by equation (9) once it is sufficiently converged. After each shape modification the flow solve is warmstarted from the original Blake airfoil periodic steady state solution and the flow is allowed to evolve for some time to establish a new periodic steady state before the cost function is calculated (compare with Figure 6). We "jump" over this unphysical adjusting period as quickly as possible by taking a bigger time step $\Delta t^* = 0.01$ for the first $N^* = 300$ steps. Once we reach our desired control window $[3, 10]$ (where we time average the objective function), we use a smaller time step $\Delta t = 0.005$ for another 1400 steps, for a total of $N = 1700$ steps covering a time interval of $[0, 10]$ for each flow solve. The corresponding adjoint equations resulting from a variable time step are given in the Appendix.

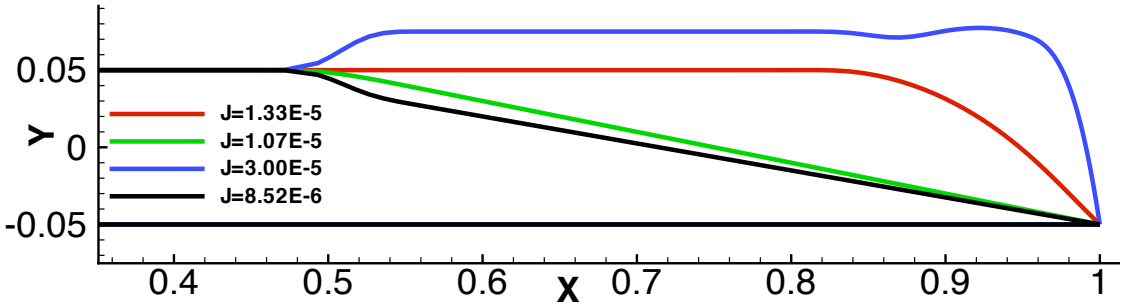

Figure 3: The initial airfoil shapes.

We start the optimization procedure from four different initial shapes, which are shown together with their objective function values (without the quadratic penalty for thickness constraint violation) in Figure 3:

1. The original Blake airfoil (in red)
2. The airfoil defined through the thickness constraint line (in green)
3. The airfoil that results from setting all fifteen design variables to their specified upper bound (in blue)
4. The airfoil that results from setting all fifteen design variables to their specified lower bound (in black)

The first three initial shapes do not violate any thickness constraints; however, the fourth one does.

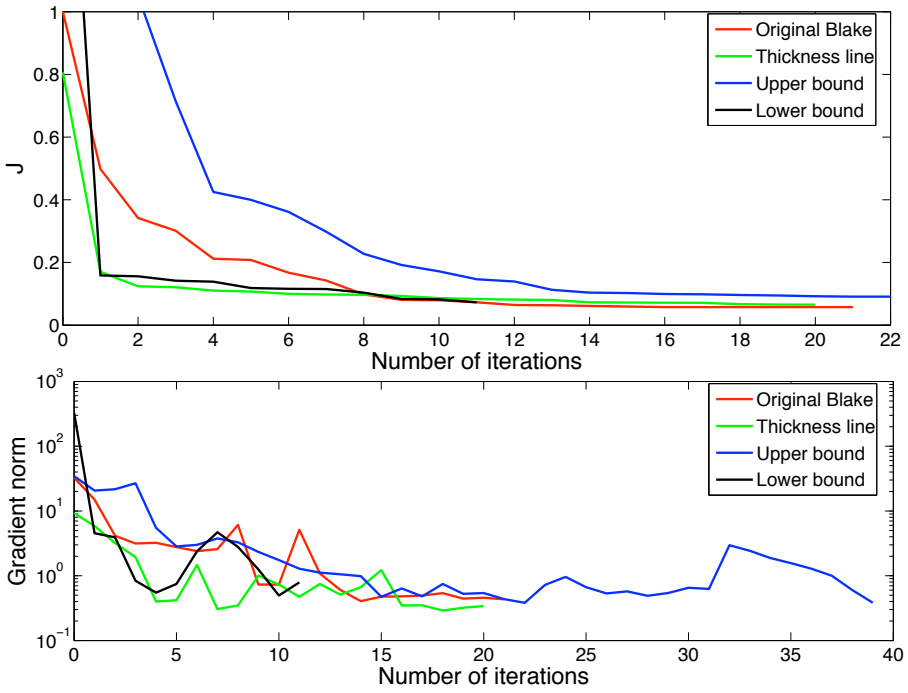

Figure 4: Convergence histories of the aeroacoustic shape design problems using fifteen design variables.

The convergence histories of these aeroacoustic shape design problems are shown in Figure 4. The objective functions are always scaled with the initial objective function value of the original Blake airfoil $J_0 = 1.33 \cdot 10^{-5}$ to make comparisons easier. One can see that all objective functions are driven to much smaller values in about two to eight design iterations and that the improvement after that is only marginal. Starting from the original Blake airfoil leads to the best airfoil in terms of total radiated acoustic power. The reduction is about 94 percent from the initial value and thus much larger than the 80 percent achieved by Marsden *et al.*[9] using five design variables. The gradient norms are only reduced by one to two orders of magnitude, implying that the optimizer did not fully converge due to stalls in the line search algorithm.

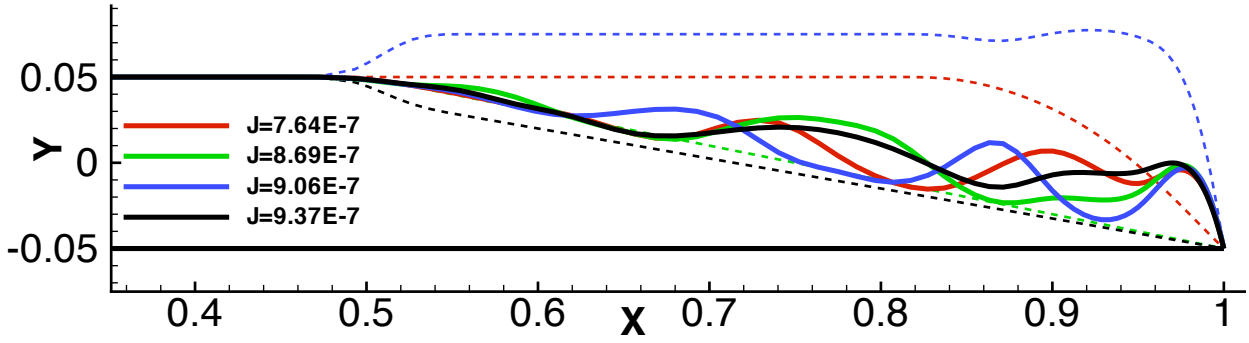

Figure 5: Final improved airfoil shapes (solid) and initial airfoil shapes (dashed).

Figure 5 shows the final improved airfoil shapes together with their objective function values (this time with the quadratic penalty for thickness constraint violation included), which are very interesting and completely unexpected. The increase in the trailing-edge angle to decrease the trailing-edge noise was also found by Marsden *et al.* and was theoretically predicted by Howe[29] for turbulent flow. However, the "wavy" part of the airfoil is a novel result and to the best of the authors' knowledge has only been reported by Rumpfkeil and Zingg[30,31] in a previous study. Presumably Marsden *et al.* did not obtain similar "wavy" shapes due to the fact that they used only five design variables and thus did not give their optimizer enough freedom to come up with these novel shapes.

	Initial			Improved		
	$\bar{C}_L$	$\bar{C}_D$	$\bar{C}_L/\bar{C}_D$	$\bar{C}_L$	$\bar{C}_D$	$\bar{C}_L/\bar{C}_D$
Original Blake	0.284	0.076	3.75	0.279	0.049	5.72
Thickness line	0.265	0.054	4.95	0.279	0.049	5.67
Upper bound	0.134	0.119	1.12	0.276	0.049	5.66
Lower bound	0.305	0.055	5.57	0.279	0.049	5.66

Table 1: A comparison of the mean lift and drag coefficients for the initial and improved airfoils.

A comparison of the mean lift and drag coefficients for the initial and improved airfoils is displayed in Table 1. We do not have to add a lift constraint or a penalty for decreased lift to the objective function since the mean lift coefficients for all improved airfoils either stay about the same or increase in comparison to their initial values. The mean drag coefficients are decreased in all cases. This means the optimizer has not only produced aeroacoustically improved airfoils, but also as a byproduct the initial airfoils have been aerodynamically enhanced.

The time histories of C_L and C_D for the original Blake airfoil before and after the optimization are shown in Figure 6. One can clearly see the unphysical adjusting period for the improved airfoil in the time interval $[0, 3]$ before it reaches its new somewhat periodic steady state. A reduced mean drag as well as reduced oscillation amplitudes for the improved airfoil are also visible.

We also tried to save computational time and storage by saving the flowfield in the control window only every second time step. We have used this approach very successfully in previous studies.[30,32] However, in this case this approach does not work very well, since the optimizer is barely able to improve the initial airfoils even slightly with this inexact gradient information.

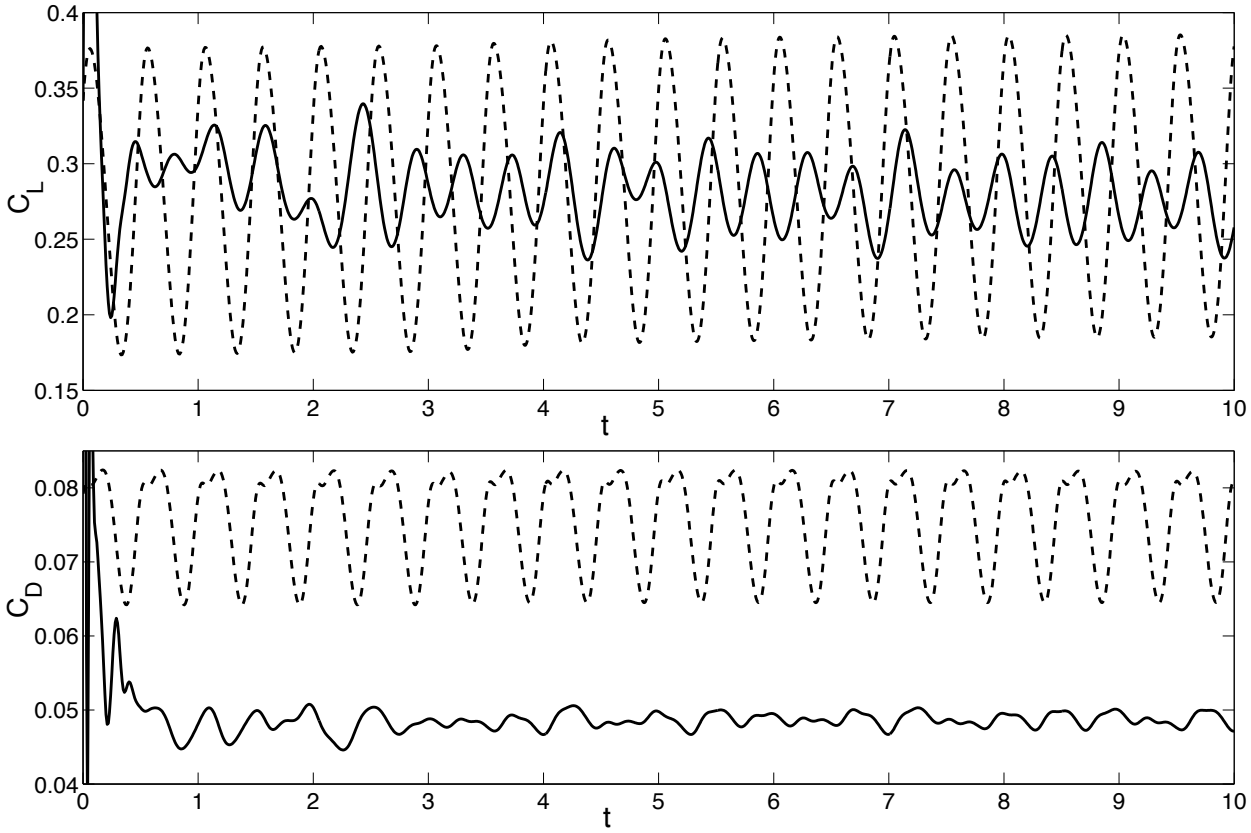

Figure 6: Time histories of C_L and C_D for the original Blake airfoil before and after optimization. The histories of the initial (dashed) and improved (solid) airfoils vs. time ($\Delta t = 0.005$) are shown.

V. Conclusion

The discrete adjoint method was successfully applied to unsteady laminar trailing edge optimization resulting in a significant reduction in the total radiated acoustic power. The resulting improved airfoils showcase very interesting and completely unexpected shapes, thereby showing the power of numerical shape optimization, which can lead to counterintuitive results. It would be very interesting to see the improved shapes tested in a wind tunnel to confirm that the predicted reduction in total radiated acoustic power is achieved in reality. The general framework presented to derive the unsteady discrete adjoint equations for optimal control can also be used for many other inherently unsteady optimization problems. Our future work will focus on the ability to modify a high-lift airfoil configuration to reduce the radiated noise while maintaining good aerodynamic performance.

Appendix

In this appendix, we derive the discrete adjoint equations in the form in which we use them to present our results. We warmstart our flow solve at $t = 0$ which implies that we know Q^0 and Q^{-1}. We also want to "jump" over the adjusting period as quickly as possible thus taking a bigger time step Δt^* for N^* time steps. Once we reach the domain where we actually want to control the problem we use a smaller time step Δt for $N - N^*$ time steps. Thus we have a total of N time steps and to keep the second-order time accuracy, the time-dependent flow solution Q^n is implicitly defined through the following unsteady residuals:

$$\mathcal{R}^n(Q^n, Q^{n-1}, Q^{n-2}, Y) := \frac{3Q^n - 4Q^{n-1} + Q^{n-2}}{2\Delta t^*} + R(Q^n, Y) = 0 \qquad \text{for} \quad n = 1, \ldots, N^*$$

$$\mathcal{R}^{N^*+1}(Q^{N^*+1}, Q^{N^*}, Q^{N^*-1}, Y) := \frac{(2\Delta t\Delta t^* + \Delta t^{*2})Q^{N^*+1} - (\Delta t + \Delta t^*)^2 Q^{N^*} + \Delta t^2 Q^{N^*-1}}{\Delta t\Delta t^*(\Delta t + \Delta t^*)} + R(Q^{N^*+1}, Y) = 0$$

$$\mathcal{R}^n(Q^n, Q^{n-1}, Q^{n-2}, Y) := \frac{3Q^n - 4Q^{n-1} + Q^{n-2}}{2\Delta t} + R(Q^n, Y) = 0 \qquad \text{for} \quad n = N^* + 2, \ldots, N.$$

The problem of minimizing the discrete objective function given by $J = \sum_{n=N^*+1}^{N} I^n(Q^n, Y)$ is then equivalent to the unconstrained optimization problem of minimizing the Lagrangian function

$$\mathcal{L} = \sum_{n=N^*+1}^{N} I^n(Q^n, Y) + \sum_{n=1}^{N} (\psi^n)^T \mathcal{R}^n(Q^n, Q^{n-1}, Q^{n-2}, Y)$$

with respect to $Q^1, \ldots, Q^N$ and $\psi^1, \ldots, \psi^N$. This leads to the following equations for ψ^n:

$$\begin{aligned}
0 &= (\psi^n)^T \nabla_{Q^n} \mathcal{R}^n + (\psi^{n+1})^T \nabla_{Q^n} \mathcal{R}^{n+1} + (\psi^{n+2})^T \nabla_{Q^n} \mathcal{R}^{n+2} && \text{for} \quad n = 1, \ldots, N^* \\
0 &= \nabla_{Q^n} I^n + (\psi^n)^T \nabla_{Q^n} \mathcal{R}^n + (\psi^{n+1})^T \nabla_{Q^n} \mathcal{R}^{n+1} + (\psi^{n+2})^T \nabla_{Q^n} \mathcal{R}^{n+2} && \text{for} \quad n = N^*+1, \ldots, N-2 \\
0 &= \nabla_{Q^{N-1}} I^{N-1} + (\psi^N)^T \nabla_{Q^{N-1}} \mathcal{R}^N + (\psi^{N-1})^T \nabla_{Q^{N-1}} \mathcal{R}^{N-1} \\
0 &= \nabla_{Q^N} I^N + (\psi^N)^T \nabla_{Q^N} \mathcal{R}^N,
\end{aligned}$$

which can be written equivalently as

$$\psi^n = \begin{cases}
-\left((\nabla_{Q^n} \mathcal{R}^n)^T\right)^{-1} \left[(\nabla_{Q^n} I^n)^T\right] & \text{for } n = N \\
-\left((\nabla_{Q^n} \mathcal{R}^n)^T\right)^{-1} \left[(\nabla_{Q^n} I^n)^T + (\nabla_{Q^n} \mathcal{R}^{n+1})^T \psi^{n+1}\right] & \text{for } n = N-1 \\
-\left((\nabla_{Q^n} \mathcal{R}^n)^T\right)^{-1} \left[(\nabla_{Q^n} I^n)^T + (\nabla_{Q^n} \mathcal{R}^{n+1})^T \psi^{n+1} + (\nabla_{Q^n} \mathcal{R}^{n+2})^T \psi^{n+2}\right] & \text{for } n = N-2, \ldots, N^*+1 \\
-\left((\nabla_{Q^n} \mathcal{R}^n)^T\right)^{-1} \left[(\nabla_{Q^n} \mathcal{R}^{n+1})^T \psi^{n+1} + (\nabla_{Q^n} \mathcal{R}^{n+2})^T \psi^{n+2}\right] & \text{for } n = N^*, \ldots, 1
\end{cases}$$

A little care must be taken in calculating derivatives of $\mathcal{R}^{N^*+1}$with respect to Q^n since the factors in front of Q^{N^*+1}, $Q^{N^*}$and Q^{N^*-1}differ slightly from the usual scheme. The gradient of J with respect to the design variables Y is then given by

$$\frac{\partial J}{\partial Y} = \frac{\partial \mathcal{L}}{\partial Y} = \sum_{n=N^*+1}^{N} \nabla_Y I^n(Q^n, Y) + \sum_{n=1}^{N} (\psi^n)^T \nabla_Y R(Q^n, Y).$$

Acknowledgments

The funding of the second author by the Natural Sciences and Engineering Research Council of Canada and the Canada Research Chairs program is gratefully acknowledged.

References

[1]Obayashi, S., *Aerodynamic Optimization with Evolutionary Algorithms*, Inverse Design and Optimization Methods, Lecture Series 1997-05, edited by R. A. V. den Braembussche and M. Manna, Von Karman Institute for Fluid Dynamics, Brussels, 1997.

[2]Jameson, A., Pierce, N. A., and Martinelli, L., "Optimum Aerodynamic Design Using the Navier-Stokes Equations," *Theoretical and Computational Fluid Dynamics*, Vol. 10, No. 1, 1998, pp. 213–237.

[3]Anderson, W. K. and Bonhaus, D. L., "Airfoil Design on Unstructured Grids for Turbulent Flows," *AIAA Journal*, Vol. 37, No. 2, 1999, pp. 185–191.

[4]Nemec, M. and Zingg, D. W., "Newton-Krylov Algorithm for Aerodynamic Design Using the Navier-Stokes Equations," *AIAA Journal*, Vol. 40, No. 6, 2002, pp. 1146–1154.

[5]Jameson, A., "Optimum Aerodynamic Design Using Control Theory," *Computational Fluid Dynamics Review, Hafez, M., Oshima, K. (eds)*, Wiley: New York, 495-528, 1995.

[6]Singer, B. A., Brentner, K. S., and Lockard, D. P., "Computational Aeroacoustic Analysis of Slat Trailing-Edge Flow," *AIAA Journal*, Vol. 38, No. 9, 2000, pp. 1558–1564.

[7]Khorrami, M. R., Berkman, M. E., and Choudhari, M., "Unsteady Flow Computations of a Slat with a Blunt Trailing Edge," *AIAA Journal*, Vol. 38, No. 11, 2000, pp. 2050–2058.

[8]Singer, B. A. and Guo, Y., "Development of Computational Aeroacoustics Tools for Airframe Noise Calculations," *International Journal of Computational Fluid Dynamics*, Vol. 18(6), 2004, pp. 455–469.

[9]Marsden, A. L., Wang, M., Dennis Jr., J. E., and Moin, P., "Optimal Aeroacoustic Shape Design Using the Surrogate Management Framework," *Optimization and Engineering*, Vol. 5(2), 2004, pp. 235–262.

[10]Broyden, C. G., "The Convergence of a Class of Double-Rank Minimization Algorithms," *Journal Inst. Math. Applic.*, Vol. 6, 1970, pp. 76–90.

[11]Fletcher, R., "A New Approach to Variable Metric Algorithms," *Computer Journal*, Vol. 13, 1970, pp. 317–322.

[12]Goldfarb, D., "A Family of Variable Metric Updates Derived by Variational Means," *Mathematics of Computing*, Vol. 24, 1970, pp. 23–26.

[13]Shanno, D. F., "Conditioning of Quasi-Newton Methods for Function Minimization," *Mathematics of Computing*, Vol. 24, 1970, pp. 647–656.

[14]Blake, W. K., "A Statistical Description of Pressure and Velocity Fields at the Trailing Edge of a Flat Strut," DTNSRDC Report 4241, David Taylor Naval Ship R & D Center, Bethesda, Maryland, 1975.

[15]Curle, N., "The Influence of Solid Boundary upon Aerodynmaic Sound," Proc. Royal Soc. Lond. A, 231:505-514, 1955.

[16]Marsden, A. L., Wang, M., and Koumoutsakos, P., "Optimal Aeroacoustic Shape Design using Approximation Modeling," Annual Research Briefs, Center for Turbulence Research, Stanford University, 2002.

[17]Wang, M., Lele, S. K., and Moin, P., "Computation of quadrupole noise using acoustic analogy," *AIAA Journal*, Vol. 34, No. 11, 1996, pp. 2247–2254.

[18]Byrd, R. H., Lu, P., Nocedal, J., and Zhu, C., "A Limited Memory Algorithm for Bound Constrained Optimization," *SIAM J. Scientific Computing 16*, Vol. 5, 1995, pp. 1190–1208.

[19]Zhu, C., Byrd, R. H., Lu, P., and Nocedal, J., "L-BFGS-B: A Limited Memory FORTRAN Code for Solving Bound Constrained Optimization Problems," Tech. Rep. NAM-11, EECS Department, Northwestern University, 1994.

[20]Pueyo, A. and Zingg, D. W., "Efficient Newton-Krylov Solver for Aerodynamic Computations," *AIAA Journal*, Vol. 36, No. 11, 1998, pp. 1991–1997.

[21]Pulliam, T. H., *Efficient Solution Methods for the Navier-Stokes Equations*, Lecture Notes for the Von Karman Institute For Fluid Dynamics Lecture Series, 1986.

[22]Isono, S. and Zingg, D. W., "A Runge-Kutta-Newton-Krylov Algorithm for Fourth-Order Implicit Time Marching Applied to Unsteady Flows," AIAA, 2004-0433, 2004.

[23]Saad, Y. and Schultz, M. H., "GMRES: A Generalized Minimal Residual Algorithm for Solving Nonsymmetric Linear Systems," *SIAM Journal on Scientific and Statistical Computing*, Vol. 7 No. 3, 1986, pp. 856–869.

[24]Meijerink, J. A. and van der Vorst, H. A., "An Iterative Solution Method for Linear Systems of which the Coefficient Matrix is a Symmetric M-Matrix," *Mathematics of Computation*, Vol. Vol. 31, No. 137, 1977, pp. 148–162.

[25]van der Vorst, H., "Bi-CGSTAB: A Fast and Smoothly Converging Variant of Bi-CG for the Solution of Nonsymmetric Linear Systems," *SIAM Journal on Scientific and Statistical Computing*, Vol. 13, 1992, pp. 631–644.

[26]Nemec, M. and Zingg, D. W., "Multipoint and Multi-Objective Aerodynamic Shape Optimization," *AIAA Journal*, Vol. 42, No. 6, 2004, pp. 1057–1065.

[27]Truong, A. H., Oldfield, C., and Zingg, D. W., "A Linear Elasticity Mesh Movement Method with an Augmented Adjoint Approach for Aerodynamic Shape Optimization," Proceedings of the 12th Annual CASI Aerodynamics Symposium, Toronto, paper 317, 2007.

[28]Truong, A. H., Oldfield, C., and Zingg, D. W., "Mesh Movement for a Discrete-Adjoint Newton-Krylov Algorithm for Aerodynamic Optimization," AIAA, 2007-3952, 2007.

[29]Howe, M. S., "The influence of surface rounding on trailing edge noise," *Journal of Sound and Vibration*, Vol. 126, No. 3, 1988, pp. 503–523.

[30]Rumpfkeil, M. and Zingg, D. W., "A General Framework for the Optimal Control of Unsteady Flows with Applications," AIAA, 2007-1128, 2007.

[31]Rumpfkeil, M. and Zingg, D. W., "Optimal Aeroacoustic Shape Design Using a Discrete Adjoint Approach," Proceedings of the 15th Annual Conference of the CFD Society of Canada, Toronto, paper 1106, pp. 221-228, 2007.

[32]Rumpfkeil, M. and Zingg, D. W., "The Remote Inverse Shape Design of Airfoils in Unsteady Flows," Proceedings of the 12th Annual CASI Aerodynamics Symposium, Toronto, paper 318, 2007.